Journal of Computer-Aided Molecular Design, 5 (1991) 335–356
ESCOM

J-CAMD 119

Development of a conformational search strategy for flexible ligands: A study of the potent μ-selective opioid analgesic fentanyl

Chiara Cometta-Morini* and Gilda H. Loew

Molecular Research Institute, 845 Page Mill Road, Palo Alto, CA 94304, U.S.A.

Received 13 July 1990
Accepted 4 December 1990

Key words: Fentanyl; AM1; CHARMm; Molecular dynamics

SUMMARY

An extensive conformational search of the potent opioid analgesic, fentanyl, was performed using the semiempirical quantum mechanical method AM1 and the CHARMm potential energy function. A combination of two procedures was used to search the conformational space for fentanyl, which included nested dihedral scans, geometry optimization and molecular dynamics simulation at different temperatures. In addition, the effect of a continuum solvent environment was taken into account by use of appropriate values for the dielectric constant in the CHARMm computations.

The results of the conformational search allowed the determination of the probable conformation of fentanyl in polar and nonpolar solvents and of three candidate conformers for its bioactive form.

INTRODUCTION

The high in vivo analgesic potency and opioid μ-receptor binding affinity of fentanyl **(1)** [1] indicate that this compound is capable of very precisely fulfilling the conformational and electronic requirements for recognition and activation of the μ-opioid receptor. Thus, the family of opioids

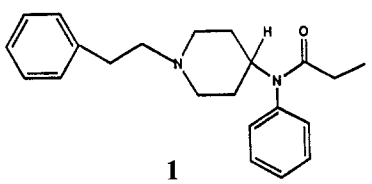

1

of which **1** is the parent compound will be a very useful addition in our continued studies to determine structural and electronic requirements for high-affinity binding and activation of the μ-receptor.

*To whom correspondence should be addressed.

Since the introduction of fentanyl in the early 1960s, extensive studies of the structure–activity relationships of the 4-anilidopiperidine class of compounds have been reported. While these studies have resulted in the discovery of numerous compounds with extremely high analgesic potency, there are a number of both experimental and theoretical gaps in current knowledge that have diminished their usefulness as templates to help elucidate the steric and electronic properties that lead to a favorable interaction with the μ-receptor.

The pharmacological studies have, by and large, used in vivo analgesia, most frequently the mouse tail flick assay, as a measure of activity. In the case of fentanyl and a number of its analogs, some of which are in clinical use like alfentanil and sufentanil, in vivo studies have been complemented by reports of binding affinity at different receptors [2,3], confirming the high affinity and selectivity of fentanyl for the μ-receptor. For most of the known fentanyls, however, the binding affinity either has not been reported or has been reported against a single labeled ligand such as fentanyl itself. Missing from our current knowledge of the pharmacology of the 4-anilidopiperidine class of compounds is therefore a systematic assessment of antagonist activity and receptor selectivity.

Studies of the structural properties of this family have taken the form of the X-ray structure determination of at least nine analogs, a number of solution NMR and IR spectroscopic investigations, and some theoretical studies of conformational profiles.

The X-ray crystallographic studies of the solid-state conformation of **1** [4] and a number of its derivatives [5–8] reveal that, in all analogs, the piperidine ring is in the chair conformation and both the 4-phenylpropanamide and the *N*-phenethyl substituents are equatorial. Information about the probable solution conformation of fentanyl in chloroform has been obtained through ^{1}H NMR and IR spectroscopy [9]. According to the ^{1}H NMR spectroscopic data, confirmed by a recent ^{13}C NMR study of fentanyl and analogs [10], the more favored conformers of **1** and the 4-anilidopiperidine derivatives are also predicted to be piperidine chairs with equatorial phenylpropanamide groups, consistent with the X-ray studies. Additional information is provided by the IR spectroscopic results, which suggest that the population of flexible piperidine twist-boat conformers with the possibility of internal hydrogen bonding, or of any internally H-bonded structure, must be low.

While these studies point to a piperidine chair conformation with both N-substituent and 4-phenylpropanamide equatorial as a likely candidate for binding to the μ-receptor, such inference would be made more convincing if confirmed by a conformational study of fentanyl followed by investigation of a series of fentanyl-type analogs with varied affinities for the μ-receptor. It is such studies which can ultimately lead to the selection of the most plausible bioactive form of this family of opioids.

A number of active conformations have been proposed for fentanyl. The earliest one, by Cheney et al. [11], was based on the assumption that fentanyl could assume a morphine-like conformation at the receptor and that either one of the phenyl groups of **1** is equivalent to the morphine phenyl group. With these assumptions, the authors used the technique of molecular mechanics to determine that the energy required for **1** to overlap with morphine was only 5.2 kcal/mol. However, subsequent structure–activity studies by Lobbezoo et al. [12] clearly showed that the underlying assumption, that one or the other phenyl group could be equivalent to that of morphine, was incorrect.

Feinberg et al. [13] proposed an 'agonist' conformation for **1** on the basis of comparison of mo-

lecular models for fentanyl itself and other very potent opioid analgesics, possessing two aromatic moieties. The suggested pharmacophore is conformationally very dissimilar from the solid-state structure, the terminal phenyl of the phenethyl moiety being twisted above the piperidine ring. This candidate active conformation was later dismissed by others [14] on account of its predictable high energy.

Similarly, Lednicer and Von Voigtlander [15] showed, with the use of Dreiding models, that fentanyl and a potent μ-selective Upjohn compound could assume conformations allowing superimposition of all salient structural features. They argued that for fentanyl such a conformation could be the pharmacologically active one but agreed that a rigorous conformational study would be needed to determine its energy requirements and its plausibility, since it was quite different from the solid and solution conformers.

Recently, an active conformation of fentanyl, which should not be a high-energy form since it is very similar to the solid and solution structure, has been proposed [14]. The only difference from the solid-state structure is in the relative position of the benzene ring and the carbonyl group in the phenylpropanamide moiety. In the solid-state structure they are in anti-, and in the proposed active conformation in syn-periplanar arrangement.

The most extensive conformational study of fentanyl published so far is the one by Tollenaere et al. [16]. In their study, the authors used the PCILO method to analyze the conformational space of fentanyl, carfentanil and compounds related to both of them, with the goal of determining the most probable receptor-recognized (i.e., bioactive) conformation for the fentanyl class of compounds. The starting structure for the conformational search was the X-ray data for nine 4-anilidopiperidines, including fentanyl itself. While the energy profiles for four of the six rotatable bonds were studied in great detail, the remaining degrees of freedom were kept fixed at their crystallographic values. Also, the search was confined to the piperidine chair with *N*- and 4-phenylpropanamide substituents equatorial. This form is, however, only one of eight possible, qualitatively different conformational domains for fentanyl-type analogs. These domains result from the combination of two piperidine ring conformations (chair and boat) and four arrangements of the 1- and 4-ring substituents (equatorial-equatorial; axial-axial; equatorial-axial; and axial-equatorial). In the pharmacophore reported, the conformation of the equatorial 4-phenylpropanamide moiety is very close to the solid-state one. However, the authors refrained from proposing an active conformation for the *N*-phenethyl moiety because of its high conformational flexibility.

More recently, two separate conformational studies of two fentanyl analogs, R30490 [17] and R26800 [18], have been published. In the first [17], the authors used a very simple potential energy calculation to locate energy minima on the R30490 conformational surface and subsequently refined the geometry optimization for key conformations using molecular mechanics. Of the eight different domains which, in analogy to fentanyl, are also accessible to R30490, the authors considered four. The results of their study show that the crystal structure conformation of the ring (chair equatorial-equatorial) is probably also conserved in the biologically active species.

The conformational study of R26800, (+)-*cis*-3-methylfentanyl [18], was performed using an empirical energy function. In analogy with the previous study, the computations favor energetically the chair equatorial-equatorial. However, once again, no complete assessment of the accessibility of the remaining conformational domains was performed.

Very recently, an article by Froimowitz [19] has appeared, in which the results of initial molecular mechanics computations of the *N*-methyl analogs of fentanyl, 3-methylfentanyl and 4-methyl-

fentanyl are presented. According to these computations, fentanyl and its *trans*-3-methyl derivative prefer the conformation with the phenylpropanamide-substituent equatorial, while the *cis*-3-methyl and 4-methyl analogs appear to favor the conformation in which the same substituent is axial, even if by less than 0.5 kcal/mol.

In view of the fact that no previous study exists in which the complete conformational space of fentanyl has been investigated, we decided that, as a first step in identification of the pharmacophore for the fentanyl class of compounds, we would perform an extensive search of the conformational space of **1** in its isolated state.

In addition, by simulating the environmental effects of polar and nonpolar solvents, we have also addressed the question of the conformers observed in IR and NMR experiments.

To accomplish these aims, we have designed a search strategy that should be an effective and efficient procedure to explore the conformational space of any drug with many internal degrees of freedom. For such intermediate-size organic molecules, two theoretical methods are most appropriate: those based on empirical energy functions and on semi-empirical quantum-mechanical procedures. It was our purpose to determine the optimum combination of these two methods to obtain a reliable description of the conformational domain of the molecule.

METHODS AND PROCEDURES

The energy computations were performed at two levels: at the empirical energy function level using the CHARMm force field [20] as available through the QUANTA [21] molecular modeling system, and at the semi-empirical quantum-mechanical level using the AM1 parametrization [22] embedded in version 5.0 of the MOPAC molecular orbital package [23]. At both levels of computation, all atoms were explicitly included. In the geometry optimizations, all geometrical parameters were allowed to vary. At the AM1 level, the geometry optimization was performed using the Broyden-Fletcher-Goldfarb-Shanno algorithm [24], which is the default method within MOPAC 5.0. A geometry was considered optimized when one of the following three criteria was satisfied: the projected change in geometry was less than 0.0001 Å; or the projected decrease in energy was less than 0.001 kcal/mol; or the gradient norm was less than the square root of the number of coordinates optimized. At the CHARMm level, the geometry optimization was performed using the Powell method [25]. Geometries were considered optimized when either of the following two

TABLE 1
DEFINITION OF CONFORMATIONAL DOMAINS FOR FENTANYL

Terminology	Ring conformation	CH_2Ch_2Ph	N(Ph)COEt
CEE	Chair	eq	eq
CEA	Chair	eq	ax
CAE	Chair	ax	eq
CAA	Chair	ax	ax
BEE	Boat	eq	eq
BEA	Boat	eq	ax
BAE	Boat	ax	eq
BAA	Boat	ax	ax

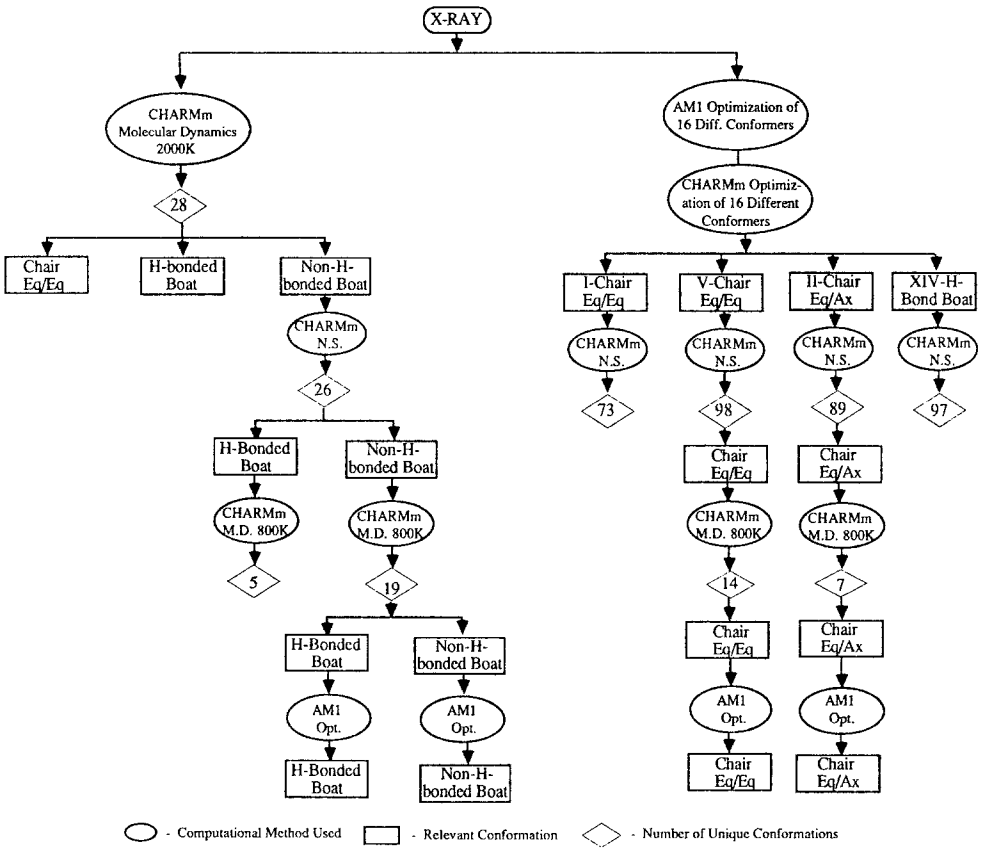

Fig. 1. Conformational search strategy for protonated fentanyl.

criteria was met: the change in energy value between two subsequent structures was less than 0.001 kcal/mol; or the root-mean-square of deviation in the geometry of two subsequent structures was less than 0.010.

The initial geometry for fentanyl, as obtained from the X-ray structure [4], was protonated since the pK_a of fentanyl (8.43) [16] indicates that the protonated form dominates in solution and we assume that this is also the pharmacologically relevant species. The protonated form was subsequently optimized with AM1 and CHARMm. The conformational search strategy used is summarized in Fig. 1. This strategy was designed in order to fully and efficiently sample the many degrees of freedom of fentanyl.

The eight different structural domains possible for fentanyl are listed in Table 1. Transition from one domain to another would most likely require overcoming a substantial energy barrier, since it involves ring inversion (e.g., CEE to CAA); change of ring conformation (e.g., CEE to BEA); or deprotonation and reprotonation (e.g., CEE to CEA). Within each domain, however, there can be significant rotational freedom of the substituents leading to many low-energy rotamers. To investigate this possibility, rotation around four of the six single bonds described by the six torsion angles, φ_1, φ_2, φ_3, τ_1, τ_2 and τ_3 as defined in Fig. 2, was performed. In addition to these variations, we have also taken into account the two possible relative orientations of the

benzene ring and the carbonyl function in the phenylpropanamide moiety: syn- and anti-periplanar, corresponding to an ω-value of 0° and 180°, respectively (Fig. 2). This variation led to boat conformers that either do or do not form internal H-bonds between the hydrogen on the quaternary nitrogen and the carbonyl oxygen. Such conformers are related by rotation around a single bond (φ_1 in Fig. 2). H-bonding is not possible in all conformers listed in Table 1.

The first step in the conformational search was the generation of optimized representative conformers for each of the eight domains listed in Table 1, further defined by $\omega = 0°$, 180°, and whether or not there is internal H-bonding (Tables 2–4).

Figure 1 represents schematically the overall strategy adopted to scan the conformational space of fentanyl. Two separate and parallel approaches were used to achieve this goal. In the first, the optimized X-ray structure was used in a molecular dynamics (MD) simulation [26–27] at high temperature (2000 K) to sample conformational space and generate structures differing in piperidine ring conformation and in the position of substituents as starting points for subsequent searches. In the MD computation, the molecule was heated to 2000 K in 0.8 ps and allowed to equilibrate for 2 ps, after which the dynamics simulation was run for 3 ps in steps of 1 fs with data collection every 0.01 ps. The high temperature was chosen in order to overcome high-energy conformational barriers, resulting in a sampling of a large portion of the conformational space. Of the 300 structures generated in the 3-ps dynamics simulation, the 50 lying lowest in potential ener-

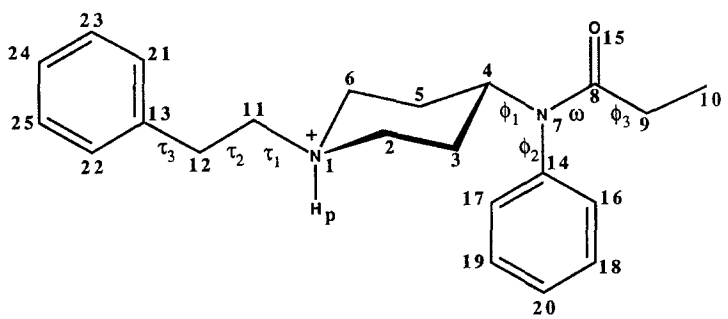

Torsion	Definition	Values assigned in rotations	X-ray [4]
φ_1	C_5-C_4-N_7-C_{14}	0°,90°,180°,−90°	−65.6°
φ_2	C_4-N_7-C_{14}-C_{16}	0°,−90°	−92.9°
φ_3	N_7-C_8-C_9-C_{10}	0°,90°,180°	177.2°
τ_1	C_{12}-C_{11}-N_1-C_6	0°,90°,180°	172.4°
τ_2	C_{13}-C_{12}-C_{11}-N_1	not varied	−170.2°
τ_3	C_{22}-C_{13}-C_{12}-C_{11}	not varied	−54.8°
ω	O_{15}-C_8-N_7-C_{14}	0°,180°	179.2°

Fig. 2. Numbering adopted and torsion definitions, together with values assigned in the nested rotations search prodecure.

TABLE 2
RESULTS OF CHARMm MOLECULAR DYNAMICS SIMULATIONS (2000 K) MOST STABLE STRUCTURE OF FENTANYL FOR EACH CONFORMATIONAL DOMAIN FOUND[a]

Structure	ΔE (kcal/mol)	φ_1	φ_2	φ_3	τ_1	τ_2	τ_3	ω	H_p--O[b] (Å)
BEA-H[c]	0.0	56.4	−151.9	54.9	−85.0	60.2	64.5	−143.6	1.72
BEA-nH[d]	8.2	−95.1	−56.3	−161.5	162.0	67.2	57.1	171.5	4.67
CAA_{ap}[e]	11.5	−166.7	2.5	143.9	−167.6	176.4	66.3	124.1	4.39
CEE_{ap}[e]	12.0	63.6	−156.3	−142.5	76.9	42.4	65.6	−56.7	4.77
CEE_{sp}[f]	15.7	−102.5	−139.3	−178.8	163.2	−177.7	64.6	6.9	6.63
BAE-nH[d]	15.8	−84.3	−45.8	−162.3	−105.6	45.5	67.5	174.5	5.92
X-ray									
CHARMm optimized	17.8	−43.9	−119.8	164.2	164.5	−172.7	−64.0	−170.4	–

[a] No structures corresponding to the other four domains CAE, CEA, BAA or BEE were found in this simulation.
[b] Distance between amine proton and carbonyl oxygen.
[c] Internal H-bonded structure.
[d] No internal H-bonding.
[e] Subscript ap means benzene and carbonyl function anti-periplanar: initial value of $\omega = 180°$.
[f] Subscript sp means benzene and carbonyl function syn-periplanar: initial value of $\omega = 0°$.

TABLE 3
AM1-OPTIMIZED FENTANYL CONFORMATIONS IN EACH OF THE EIGHT STRUCTURAL DOMAINS

Conformer	$\Delta(\Delta H_f)$ (kcal/mol)	φ_1	φ_2	φ_3	τ_1	τ_2	τ_3	ω	H_p--O (Å)
XIV - BEA-H	0.0	81.9	−105.3	−176.5	68.0	172.4	−74.4	−176.8	2.0
V - CEE	1.0	115.1	−94.1	179.9	77.3	177.4	−62.7	−177.0	3.9
VII - CAE	2.6	117.6	−92.0	−179.9	−170.5	163.0	−82.4	−179.9	5.4
II - CEA	3.2	−174.0	−96.7	−158.7	178.7	−168.5	−54.8	166.3	4.9
I - CEE	3.2	−61.1	−84.1	178.7	167.3	−171.9	−62.6	178.6	6.0
VI - CEA	4.4	−6.0	−80.7	−179.9	79.2	179.1	−68.1	−177.9	5.6
IV - CAA	4.8	−163.8	−105.0	−174.9	−157.9	176.6	−75.5	177.3	4.3
III - CAE	5.1	−61.4	−86.1	178.8	−160.6	171.9	−66.4	−179.7	6.1
X - BEA-nH	6.2	−25.4	−98.2	178.1	172.9	−176.2	−73.5	−175.0	4.9
VIII - CAA	6.3	9.4	−82.8	179.6	−64.2	−168.5	−69.6	−179.2	6.0
IX - BEE	6.7	−116.3	−80.0	179.2	164.5	−171.9	−64.6	178.7	5.2
XIII - BEE	7.4	76.3	−82.3	177.5	69.2	171.4	67.7	174.7	4.3
XI - BAE	9.9	−117.9	−81.7	180.0	−124.2	−179.0	−66.0	179.0	5.6
XV - BAE	10.2	88.1	−92.9	177.2	105.9	−170.2	−54.8	180.0	5.6
XII - BAA	11.5	177.5	−56.3	−89.2	−100.9	177.8	−68.6	174.0	4.4

Note: The following pairs of conformers are related through variation of φ_1: I, V; II, VI; III, VII; IV, VIII; IX, XIII; X, XIV; XI, XV. Conformer XII does not have a partner since the optimization of the corresponding structure (inverted boat axial-axial) failed to converge due to steric crowding of the substituents.

gy were fully optimized with CHARMm. Subsequent clustering according to similarity in the seven torsional angles listed in Fig. 2 yielded 28 unique structures.

In the second approach, explicit conformers representing the eight possible domains of fentanyl were generated and the structures thus obtained were fully optimized with both AM1 and CHARMm.

In the second step, the rotational profile of the substituents in four of the eight domains was examined, excluding from consideration those with the *N*-phenethyl moiety in an axial position. The reason for eliminating them is that in each case they were higher in energy than their *N*-equatorial counterpart and there is no evidence from ongoing studies of other fentanyl analogs that they are involved as the 'bioactive form' at the receptor.

As the starting point in this procedure, as shown in Fig. 1, we selected the lowest-energy form of the conformers in each of these four domains, whether it came from the MD search or the generation of explicit starting structures of each type. Thus, the conformers chosen (Fig. 1) were respectively the lowest-energy representatives of the four following classes: (a) piperidine ring boat with internal hydrogen bonding (XIV, H-bonded boat); (b) piperidine ring boat without internal hydrogen bonding (non-H-bonded boat); (c) piperidine chair with both substituents in equatorial arrangement (V, chair eq/eq); and (d) piperidine chair with *N*-phenethyl substituent equatorial and phenylpropanamide substituent axial (II, chair eq/ax). The fifth conformer is the one corresponding to the solid-state structure of fentanyl (I, chair eq/eq).

TABLE 4
RESULTS OF CHARMm REOPTIMIZATION OF 16 AM1-OPTIMIZED CONFORMERS OF FENTANYL

Conformer	$\Delta(\Delta E)$ (kcal/mol)	φ_1	φ_2	φ_3	τ_1	τ_2	τ_3	ω	H_p--O (Å)
XI - BEA-H[a]	0.0	−108.8	−33.8	−159.8	−153.6	−178.2	−65.8	−178.2	1.8
V - CEE[b]	0.6	89.5	−122.3	166.3	76.7	−178.6	−65.8	−147.3	1.8
XIV - BEA-H	0.8	110.2	−142.9	161.8	69.3	−177.4	−65.8	179.4	1.8
X - BEA-H[c]	0.8	54.8	−150.6	148.5	154.8	−172.6	−66.0	−147.4	1.8
II - CEA	1.8	−158.8	−128.1	174.8	164.3	−174.2	−64.6	−128.3	4.1
IV - CAA	2.5	−156.9	−127.2	175.1	−159.0	−179.2	−66.0	−129.5	3.3
VII - CAE	2.7	88.0	−121.8	171.3	−172.8	177.9	−67.9	−143.0	5.0
XII - CEA[d]	5.5	−167.1	−37.4	−75.8	−66.4	−176.2	−65.4	−159.0	5.0
IX - BEE	5.8	−117.2	−32.8	−162.2	154.7	−173.3	−64.0	−176.3	4.2
VI - CEA	7.3	25.6	−70.5	−163.2	70.5	−179.9	−66.6	157.8	5.5
VIII - CAA	7.7	26.2	−70.7	−163.1	−71.4	−174.6	−65.9	157.7	5.9
I - CEE	9.4	−73.3	−68.3	−165.3	164.3	−173.9	−65.6	145.2	5.6
III - CAE	9.5	−72.6	−68.3	−165.5	−166.3	−179.3	−66.2	144.9	6.1
XV - BAE	14.0	94.1	−35.2	−166.8	64.7	180.0	−64.5	−171.1	5.9
XIII- BEE	14.9	93.8	−35.2	−166.9	74.9	−177.9	−66.0	171.2	4.3

[a] Conformer XI, which was optimized to a boat axial-equatorial with AM1 rearranged to a boat equatorial-axial during the CHARMm optimization.

[b] The chair conformation is flattened in the CHARMm structure to allow the formation of internal hydrogen bonding.

[c] Conformer X, which was optimized as a boat equatorial-axial without internal hydrogen bonding with AM1, rearranged to a boat equatorial-axial with internal hydrogen bonding during the CHARMm minimization.

[d] Conformer XII, which was optimized as a boat axial-axial with AM1, rearranged to a chair equatorial-axial during the CHARMm minimization.

As indicated in the flow chart, for each of these five optimized structures we performed nested rotations to study the conformational profile of the *N*-phenethyl and the phenylpropanamide substituents at the CHARMm level. To this end, five of the seven torsion angles of fentanyl, namely, φ_1, φ_2, φ_3, τ_1 and ω, were varied. The two remaining torsions, τ_2 and τ_3, were initially assigned their crystallographic values [4], but allowed to optimize. The values of each torsion angle in the study as well as their definition are given in Fig. 2. We decided to use a dihedral-angle resolution of 90° for φ_1, φ_2, φ_3 and τ_1 and of 180° for ω. For φ_2, we considered only the two values 0° and −90° corresponding to an arrangement of the phenyl ring parallel and perpendicular respectively to the plane bisecting the piperidine ring. The values assigned in the conformational search (see Fig. 2) correspond to big increments in the torsion values but are justified by comparison with the values assumed in the solid-state structure (Fig. 2), and by considering that complete geometry optimization of all the parameters is allowed throughout the computation.

For each one of the five starting conformers, 144 structures were generated and their energy determined through simultaneous relaxation of φ_1, φ_2, φ_3, τ_1 and ω and full optimization of the remaining degrees of freedom. The structures obtained from each of the five nested rotation searches were compared (clustered) according to similarity in the seven dihedral angles given in Fig. 2. After clustering, all conformers (except the lowest energy one) for which the values of the torsions were similar to within a root-mean-square deviation (RMSD) of 10 were discarded. In this way, we could reduce the number of conformers from 144 per nested rotation to a number ranging between 98 and 26, depending on the search results (see Fig. 1). Comparison of the conformers obtained from the five nested rotation searches allowed us to extract the lowest-energy hydrogen-bonded boat, non-hydrogen-bonded boat, chair equatorial-equatorial and chair equatorial-axial structures (Table 5).

In a third step in our analysis, we investigated whether lower-energy forms of each of these four types of conformers existed. This refinement was made using MD at 800 K. This temperature was selected for the MD simulation because we observed, through testing different values, that such a temperature is high enough to induce conformational mobility of the side chains without inducing a change in the ring conformation from chair to boat or vice versa. In each of the four MD computations, the starting structure was heated to 800 K in 2 ps, then allowed to equilibrate for 2 ps. The actual simulation was run for 2 ps in steps of 1 fs with data collection every 0.01 ps. The 196

TABLE 5
LOWEST-ENERGY ROTAMERS OF FENTANYL IN THREE MOST FAVORED STRUCTURAL DOMAINS FROM CHARMm-OPTIMIZED NESTED ROTATIONS SCANS

Conformer	ΔE (kcal/mol)	φ_1	φ_2	φ_3	τ_1	τ_2	τ_3	ω	H_p--O (Å)
BEA-H	0.0	112.0	−142.9	48.3	141.6	56.9	66.6	−145.4	1.7
BEA-nH	8.8	−92.9	−54.7	−166.3	163.5	67.5	−55.5	154.0	4.6
CEA_{ap}	10.9	−157.9	−126.9	55.8	165.7	−175.7	−63.6	−133.1	4.0
CEE_{ap}	12.4	−95.6	−116.5	173.3	155.9	−44.4	−62.0	−153.4	5.9
CEE-I[a]	19.5	−73.3	−68.3	−165.3	164.3	−173.9	−65.6	145.2	5.6

[a] CHARMm-optimized solid-state structure.

TABLE 6
REFINEMENT OF LOWEST-ENERGY CONFORMERS OBTAINED FROM NESTED ROTATIONS USING 800 K MD SIMULATION (CHARMm)

Conformer	ΔE (kcal/mol)	φ_1	φ_2	φ_3	τ_1	τ_2	τ_3	ω	H_p--O (Å)
BEA-H	0.0	174.2	−38.2	−59.2	134.8	54.6	66.8	150.5	1.7
CEA_{ap}	5.1	−158.1	−126.9	56.1	154.6	−41.4	−63.0	−133.2	4.0
BEA-nH	8.8	−91.3	−53.0	−167.3	−83.9	61.3	63.6	153.5	4.4
CEE_{ap}	12.1	−87.2	−113.6	169.7	155.9	−39.9	−65.8	−149.9	5.8
CEE-I[a]	20.4	−73.3	−68.3	−165.3	164.3	−173.9	−65.6	145.2	5.6

[a] CHARMm-optimized X-ray structure.

TABLE 7
RESULTS OF AM1 OPTIMIZATION OF LOWEST-ENERGY CONFORMERS FROM 800 K MD SIMULATIONS (CHARMm)

Conformer	$\Delta(\Delta H_f)$ (kcal/mol)	φ_1	φ_2	φ_3	τ_1	τ_2	τ_3	ω	H_p--O (Å)
CEA_{ap}	0.0	117.6	−112.8	82.7	163.8	−55.0	−116.0	−177.0	4.2
BEA-H	0.1	138.2	111.5	−81.4	138.9	62.0	89.8	173.8	2.0
CEE_{ap}	3.3	−92.8	−118.2	167.5	160.0	−56.2	111.7	172.0	5.7
BEA-nH	8.7	−117.6	113.3	−175.0	−107.6	68.6	65.2	−177.2	4.7
CEE-I[a]	5.4	−61.1	−84.1	178.7	167.3	−171.9	−62.6	178.6	6.0

[a] AM1-optimized X-ray structure.

TABLE 8
RESULTS OF CHARMm COMPUTATIONS WITH DIFFERENT VALUES OF THE DIELECTRIC CONSTANT

	CHARMm energy (ΔE, kcal/mol)		
Structure	$\varepsilon = 1$	$\varepsilon = 78$[a]	$\varepsilon = 4.8$[b]
CEE-V-β	11.6[c]	0.0	–
CEE-α	12.1	0.1	0.0
CEE-I-α[d]	20.4	2.2	3.2
CEA	5.1	3.9	1.7
BEA-H	0.0	4.3	1.4
BEA-nH	8.8	7.9	5.7

[a] Dielectric constant for water at 25°C [28].
[b] Dielectric constant for chloroform at 20 °C [28].
[c] Flattened ring structure.
[d] CHARMm-optimized X-ray structure of **1**.

structures generated in this way were fully optimized with CHARMm and then clustered according to similarities in the torsion angles. The clustering process drastically reduced the number of conformations to be analyzed to 5–19 unique structures.

The four lowest-energy conformers obtained from the CHARMm MD simulations for each of the four classes (hydrogen-bonded boat; non-hydrogen-bonded boat; chair equatorial-equatorial; chair equatorial-axial) (Table 6), were then reoptimized with AM1 (Table 7) and the energy ordering obtained by the two methods compared.

In the search strategy just described, which led to identification of the four lowest-energy conformers, all CHARMm energy computations were performed assuming the molecule to be in its isolated state (i.e., with a value of the dielectric constant equal to one). Then, as a first approximation to the effect of a solvent environment, we reoptimized the lowest-energy conformation of each of the four types as well as the conformation corresponding to the X-ray structure, using CHARMm with two different values of ε, namely, the dielectric of water ($\varepsilon = 78$) [28] and the dielectric of chloroform ($\varepsilon = 4.8$) [28] (Table 8).

RESULTS

The results of the first step of conformational analysis, obtaining representative low-energy conformers of each of the eight domains and two sub-domains by two different search strategies, are given in Tables 2–4.

Shown in Table 2 are the results obtained by high-temperature MD. Four different conformational domains were sampled. In order of appearance on the time scale, these are: $(CEE)_{ap}$, the chair equatorial-equatorial, non-hydrogen-bonded, anti-periplanar; $(CEE)_{sp}$, the chair equatorial-equatorial, non-hydrogen-bonded, syn-periplanar; (BAE-nH), the boat axial-equatorial, non-hydrogen-bonded, anti-periplanar; (BEA-nH), the boat equatorial-axial, non-hydrogen-bonded anti-periplanar; (BEA-H), the boat equatorial-axial, hydrogen-bonded, anti-periplanar; and $(CAA)_{ap}$, the chair axial-axial, non-hydrogen-bonded, anti-periplanar. No conformer corresponding to the other four domains, CAE, CEA, BAA or BEE, was found.

Of the 28 unique structures obtained from the MD computations, we report in Table 2 the CHARMm energy and torsion values for the most stable one of each conformational domain found. As can be seen, the lowest-energy structure is a boat with internal hydrogen bonding (BEA-H), the lowest lying chair equatorial-equatorial $(CEE)_{ap}$ being 12.0 kcal/mol higher in energy. The greater stability of BEA-H can be attributed mostly to the formation of the internal hydrogen bond, which is not allowed in the CEE_{ap} conformer. A measure of the stabilizing effect of the hydrogen bond can be obtained from the energy difference between BEA-nH and BEA-H, which is 8.2 kcal/mol.

Interestingly, the lowest-lying CEE structure ($\triangle E = 12.0$ kcal/mol) is 5.8 kcal/mol lower in energy than the optimized X-ray structure, and differs from it mainly in the conformation assumed by the phenethyl side chain, as can be seen from the values of the torsion angle τ_2 in Table 2.

Although the MD computations were valuable in sampling the conformational space in the time utilized, they did not span it completely. The four conformational domains, which were not spanned in the search (CEA, CAE, BEE, BAA), could only have been accessed from the CEE starting structure through a bond-breaking process. This, however, is not allowed by the CHARMm potential energy function, which is of the molecular mechanics type. We, therefore,

generated 16 different conformations for fentanyl as described in the methods section, and fully optimized them using AM1. The results of these optimizations are reported in Table 3. It must be noted that the 16 conformers generated represent two examples of each of the 8 domains and are pairwise related through a rotation of φ_1 around the C_6–N_7 single bond, a rotation which changes the position of the carbonyl function with respect to the protonated nitrogen.

As in the case of the MD computation, the lowest lying energy conformer is a boat with internal hydrogen bonding (structure XIV). However, the AM1 computations make the CEE structure (V) the second lowest lying at only 1.0 kcal/mol from the most stable BEA-H structure, in contrast to the CHARMm results, where it was the fourth conformer with an energy difference of 12.0 kcal/mol. The two conformers with piperidine ring chair and equatorial-equatorial arrangement of the substituents (I and V in Table 3) differ in the value of φ_1, which defines the orientation of the anilido phenyl with respect to the piperidine ring. In conformer I, the anilido phenyl is in the α- and in conformer V in β-orientation (see Ref. 14, p. 298 for definition). The next five most stable conformers by the AM1 optimization all have a chair piperidine ring, and differ only in the arrangement of the ring substituents.

In an attempt to reduce the disparity between the AM1 and MD results, the 16 different conformations optimized using AM1 were also optimized using CHARMm (Table 4). Comparison of Tables 3 and 4 reveals that, while both AM1 and CHARMm optimized conformers have similar lowest-energy forms and the second-lowest energy form for both is now the same – a CEE structure with a very small energy difference – in general CHARMm optimization still favors low-energy boat forms much more than AM1. It should be noted that, in the CHARMm optimization, the piperidine ring in conformer V (CEE) rearranged to assume a conformation which can be described as a flattened chair. This distortion from the ideal chair conformation allows the formation of an internal hydrogen bond between the carbonyl oxygen and the hydrogen on the quaternary nitrogen.

In the next level of refinement, the conformational profile with respect to variation in selected torsion angles of a limited set of structures in each of four domains was investigated. Comparison of the CHARMm optimization results (Table 4) with the AM1 results (Table 3) allowed the selection of structures in three of the four domains with the *N*-phenethyl substituent equatorial, BEA, CEE, and CEA, for the next level of conformational analysis. The BEE structure was not included because it was more than 5 kcal/mol above the minimum energy structure by both methods. The structures were selected as follows: structure XIV as the lowest-energy representative of the piperidine boat with internal hydrogen bonding (BEA-H); structure V as the lowest-energy representative of the piperidine chair equatorial-equatorial class (CEE); and structure II as the lowest-energy representative of the piperidine chair equatorial-axial class (CEA). We also decided to study the rotational profile of structure I (CEE-X-ray) with piperidine chair and equatorial-equatorial substituents, in spite of its relatively high CHARMm energy, because it corresponds to the solid and probable solution structure of fentanyl.

In addition to these four conformers obtained from CHARMm reoptimization of AM1 optimized structures, we included in the nested rotations study the lowest energy non-hydrogen-bonded boat obtained from the MD computation (BEA-nH, Table 2).

Analysis of the unique conformations obtained from the nested rotations allowed us to select the lowest-energy rotamers for each of the four structures considered. These results are given in Table 5. A detailed analysis of the results of the two nested rotations studies, starting from con-

formers I and V, respectively, showed that in both cases the low-energy chair equatorial-equatorial structures obtained presented an α-arrangement of the anilido phenyl. The absence of CEE structures with a β-arrangement can be attributed to overestimation by the CHARMm energy function of the electrostatic interactions in vacuo. Due to this overestimation in the energy optimization process, the piperidine ring undergoes either distortion from the chair to a flattened chair conformation or rearranges from chair to boat in order to favor the formation of an internal hydrogen bond. The boat equatorial-axial hydrogen-bonded (BEA-H) remains the lowest-energy conformer, with the best chair equatorial-equatorial $(CEE)_{ap}$ still 12.4 kcal/mol above it but still lower than the CEE conformer derived from the X-ray structure.

All conformers had an anti-periplanar arrangement of the phenyl and carbonyl group, with the syn-periplanar arrangement higher in energy. For example, CEE_{sp} was 6.9 kcal/mol higher in energy than the lowest-energy CEE_{ap}. Similarly, the lowest-energy CEA_{sp} lies 7.2 kcal/mol above the lowest-energy CEA_{ap}. Thus, we decided not to further pursue the conformational study of the syn-periplanar arrangement. However, two more levels of refinement of the four conformers given in Table 5 were investigated.

MD simulations at 800 K of each conformer were performed, and 196 structures generated and optimized. The resulting lowest-energy form of each is presented in Table 6 and Fig. 3. We see that MD simulation led to a different ordering of energy and different conformations. The MD simulation of the lowest-energy optimized chair equatorial-axial obtained from the nested rotations search led to a still lower energy form, 6.6 kcal/mol lower in energy than the starting conformation. Comparison of the CEA structures (Fig. 4) before and after MD simulation reveals an almost identical overlap of the piperidine ring, of the phenylpropanamide moiety, and of the C_α

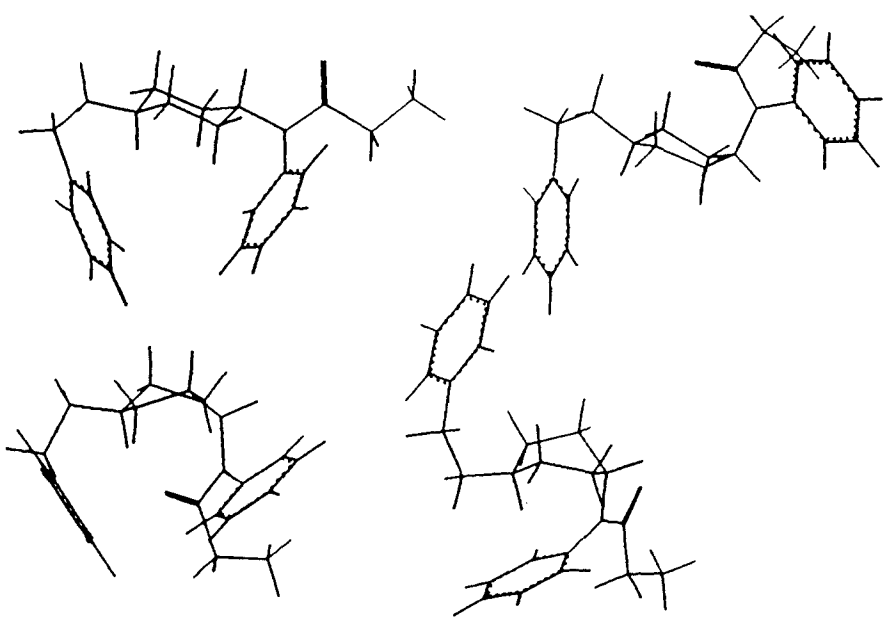

Fig. 3. Lowest-energy rotamers obtained from low-temperature CHARMm MD: chair equatorial-equatorial (upper left); chair equatorial-axial (upper right); boat equatorial-axial hydrogen bonded (lower left); boat equatorial-axial non-hydrogen bonded (lower right).

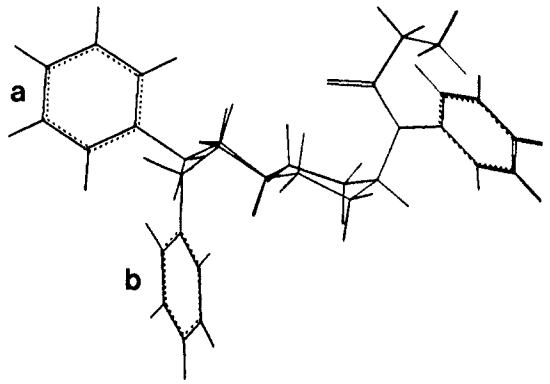

Fig. 4. Superimposition of two low-energy CEA structures: one from a nested rotation search (a) and the other (b) after low-temperature MD simulations of the first.

and C_β of the phenethyl side chain. The only difference is in the position of the benzene ring in the phenethyl moiety. A similar orientation is assumed by the same phenyl ring in the lowest-energy chair equatorial-equatorial (CEE in Table 6). Superimposition of the CEE and of the optimized solid-state conformations (Fig. 5) shows a very good overlap of the piperidine ring, a fairly good overlap of the phenylpropanamide function, but a completely different orientation of the phenyl ring of the phenethyl substituent, due mainly to a different value of the torsion angle τ_2 ($\tau_2 = -39.9°$ in CEE and $\tau_2 = -173.9°$ in the CHARMm optimized solid-state structure). This results in an arrangement of the phenethyl substituent, in which the phenyl ring is bent back towards the piperidine ring and almost parallel to the second aromatic moiety.

As a final step, the four lowest-energy conformations in Table 6 were reoptimized with AM1 (Table 7). This resulted in a rearrangement of the stability order, with the chair equatorial-axial being as stable as the boat equatorial-axial hydrogen bonded. All energy differences are much smaller using AM1 and the chair equatorial-equatorial (CEE) is within an accessible energy range. By both methods, the boat equatorial-axial non-hydrogen-bonded is too high in energy to be considered as a candidate active conformer.

Both AM1 and CHARMm predict the lowest-energy conformer to be a hydrogen-bonded boat

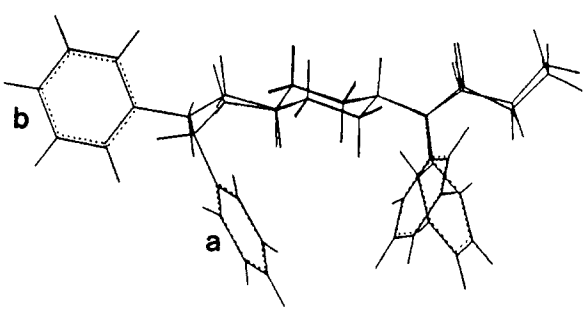

Fig. 5. Superimposition of lowest-energy chair equatorial-equatorial from low-temperature MD (a) with CHARMm optimized solid-state structure (b).

with the phenethyl substituent equatorial and the phenylpropanamide substituent axial. This conclusion is in clear contrast with the available spectroscopic data, which predict the chair equatorial-equatorial to be the most stable conformation in solution and seem to rule out any significant contribution from the hydrogen-bonded boat conformation [9].

To address this discrepancy, it was necessary to investigate the effect of the solvent environment on the energy ranking of the different conformers. Both the ^{1}H NMR and the IR spectra of fentanyl were recorded in chloroform [9]. Thus, the effect of this solvent was simulated by changing the value of the dielectric constant ε from 1 to 4.8 (dielectric constant of chloroform at 20°C [28]) and reoptimizing the structures using CHARMm. In addition, we simulated the effect of an aqueous environment by embedding the structures in a continuum with dielectric constant of 78, the dielectric of water at 25°C [28], although, to our knowledge, no spectroscopic study of fentanyl in water has been published. We also decided to reoptimize with CHARMm, and a changed value of the dielectric constant, the CEE conformer with a β-arrangement of the anilido phenyl (V in Tables 3 and 4), to verify our assumption that the failure of the nested-rotations search in locating any low-energy conformer with such an arrangement was due to overestimation of the electrostatic interactions by CHARMm in vacuo.

The results of the CHARMm energy minimization with different values of the dielectric constant are given in Table 8. As can be seen, even such a simple approximation of the effect of the solvent environment suffices to reverse the rank ordering of energy completely. According to these results, the most stable conformation of protonated fentanyl in both water and chloroform is chair equatorial-equatorial (CEE in Table 8). Two CEE conformers, one with phenylpropanamide in α- (CEE-α) and the other with phenylpropanamide in β-arrangement (CEE-V-β), are now equal in energy. This result confirms our supposition that in vacuo overestimation of the electrostatic interaction by the CHARMm potential energy function is responsible for not finding any CEE conformer with β-arrangement of the anilido phenyl. The conformation (Fig. 5) corresponding to the solid-state structure (CEE-I-α) is second in stability in water. In chloroform, the second stable structure is the hydrogen-bonded boat closely followed by the chair equatorial-axial.

DISCUSSION

Discussion of methods

Our study has shown that a combined use of potential energy function and quantum-mechanical methods is recommended in order to study the conformational mobility of small drug molecules. The two methods complement each other.

Potential energy function methods such as CHARMm have the advantage of greater computational speed and as such allow extensive conformational searches, which involve the generation of a great number of different conformations. Also, such methods, being embedded in a powerful molecular modeling system, allow fast analysis and comparison of the generated conformers – no small task. A great advantage of the CHARMm method is the possibility of using it coupled with 'classic' conformational search techniques (i.e., nested dihedral scans) and with state-of-the-art methods (MD simulations).

The main disadvantage of the CHARMm method is in the quality of the energy function. In our study we have noticed, through comparison with the AM1 results, a clear overestimation of

the electrostatic interactions. The weight of this kind of interaction in the potential energy is particularly high in our case since the molecule considered is charged.

In this respect, it is worthwhile pointing out that in the CHARMm computations the same net atomic charges were used for all different conformers, since the value assigned to them only depends on the connectivities of the atoms [29]. Comparison of the net atomic charges obtained with AM1 for the four lowest-energy conformers and for the solid-state structure shows that, in general, changes in conformation do not affect the charges significantly (Table 9). The biggest variations occur with the amide nitrogen (N_7), oxygen function (O_{15}), and proton (H_p). With respect to the AM1 net atomic charges, the charges used by CHARMm are, overall, too positive for the carbon atoms, amide nitrogen and oxygen. Moreover, the charge on the amine nitrogen (N_1) is too negative and that on the proton too positive. This results in a strong polarization of the N_1-H_p bond and certainly favors the formation of a hydrogen bond between H_p and the oxygen of the

TABLE 9
NET ATOMIC CHARGES FOR HEAVY ATOMS AND PROTON FROM AM1 AND CHARMm COMPUTATIONS FOR THE FOUR LOWEST-LYING CONFORMERS AND FOR X-RAY STRUCTURE[a]

	AM1					CHARMm
	X-ray I	CEE	CEA	BEA-H	BEA-nH	
N_1	−0.009	−0.009	0.007	−0.011	−0.002	−0.368
C_2	−0.121	−0.119	−0.133	−0.116	−0.123	0.091
C_3	−0.208	−0.216	−0.192	−0.199	−0.196	0.018
C_4	0.036	0.041	0.041	0.038	0.029	0.091
C_5	−0.208	−0.197	−0.193	−0.193	−0.198	0.018
C_6	−0.120	−0.121	−0.130	−0.114	−0.124	0.049
N_7	−0.322	−0.311	−0.297	−0.297	−0.342	−0.228
C_8	0.322	0.317	0.333	0.339	0.311	0.171
C_9	−0.166	−0.167	−0.173	−0.171	−0.167	−0.180
C_{10}	−0.210	−0.211	−0.214	−0.215	−0.211	0.105
C_{11}	−0.131	−0.124	−0.120	−0.120	−0.121	0.098
C_{12}	−0.130	−0.142	−0.144	−0.141	−0.136	0.049
C_{13}	−0.119	−0.147	−0.143	−0.129	−0.131	−0.077
C_{14}	0.018	0.025	0.011	0.009	0.015	0.000
O_{15}	−0.350	−0.358	−0.430	−0.450	−0.335	−0.275
C_{16}	−0.139	−0.133	−0.131	−0.133	−0.141	−0.078
C_{17}	−0.139	−0.155	−0.139	−0.135	−0.182	−0.078
C_{18}	−0.120	−0.113	−0.114	−0.114	−0.118	−0.095
C_{19}	−0.119	−0.118	−0.113	−0.113	−0.114	−0.095
C_{20}	−0.112	−0.116	−0.110	−0.108	−0.109	−0.096
C_{21}	−0.112	−0.135	−0.131	−0.144	−0.130	−0.093
C_{22}	−0.126	−0.125	−0.129	−0.116	−0.132	−0.093
C_{23}	−0.116	−0.119	−0.119	−0.125	−0.117	−0.096
C_{24}	−0.116	−0.115	−0.117	−0.119	−0.115	−0.096
C_{25}	−0.102	−0.102	−0.104	−0.108	−0.104	−0.096
H_p	0.238	0.251	0.238	0.286	0.251	0.380

[a] See Fig. 2 for atom numbering.

carbonyl function. This could explain the persistence of an internally hydrogen-bonded boat structure as the lowest-energy conformer in all CHARMm computations in the gas-phase approximation.

Due to the better quality of the energy function, the AM1 computations have been used by us mainly as a control of the CHARMm results. It is through comparison of the results obtained with both methods for the structures representative of the different conformational domains that we could ultimately decide on the set of candidate active conformers to be further investigated. Until an increase in computer speed will make extensive conformational searches of medium-sized molecules possible with semi-empirical quantum-mechanical methods, we believe that a suitable role of the latter kind of computations is in calibration based on energy orderings and structure optimizations in order to check the results of the potential energy function method at decisive stages of the search process.

A comment is appropriate here about the performance of the two different conformational search techniques adopted: systematic dihedral search, and MD. In theory, the dihedral-search method can promise an adequate search of the entire conformational space. In practice, though, we had to limit the number of torsions to be varied and also the number of increments in the dihedral scan to make the search amenable. We are quite confident of having covered all possible minima for the five torsions scanned, in spite of the relatively large increments used, because we allowed for full geometry optimization. We, of course, cannot say the same for the two torsions that we did not vary (τ_2 and τ_3). As a result, in all nested rotations searches but one, these two torsion angles, although free to vary, maintained the value they had in the starting structure. A notable exception is given by the set of conformers corresponding to the lowest chair equatorial-equatorial. The values assumed by τ_2 and τ_3 in this set substantially differ from the values in the starting structure for the dihedral scan.

In the MD computations, on the other hand, no limitations in the number of parameters to be varied was imposed. Consequently, both in the high- and low-temperature MD simulation, all dihedral angles assumed values different from those of the starting structure.

On this ground, MD seems to be a better tool for sampling the conformational space, especially because variation of the temperature of the simulation allows control over the barrier height that the molecule can climb (i.e., over the number of conformational domains to be spanned).

However, if MD is the only search tool used, care must be taken that the simulation is run for a sufficiently long time and at a sufficiently high temperature to sample all possible conformational domains.

In the case of our high-temperature MD computation, the length of the simulation was sufficient to cover all conformational domains accessible from the starting structure with the particular energy function used. In general, it is hard to predict in advance how much of the conformational domain will be covered and what subsequent simulations with either different starting structures or at different temperatures might be necessary.

As we noted from the results of our high- and low-temperature MD simulations, the high-temperature run covered more of the conformational space but generated a larger number of high-energy conformers, while the low-temperature run generated very few significantly different geometries. However, both types of run were successful in finding new local minima.

Discussion of results

The conformational search strategy used allowed us, in a hierarchy of refinement, to locate 439 fully optimized, different local minima for fentanyl and to definitely select a low-energy form from each type of structural domain.

The results of the computations indicate that, for fentanyl in its isolated state, the most stable conformation is the internally hydrogen-bonded boat (BEA-H). This conformation is definitively more stable according to the CHARMm results and less so from the AM1 results in which the chair equatorial-axial is equally stable as the H-bonded boat. Both methods predict a higher energy for the lowest-energy chair equatorial-equatorial (CEE), while the optimized solid-state form of CEE is even higher in energy.

The results of the isolated state computations favoring the boat clearly show a discrepancy with solution spectroscopic data [9,10]. Also, pharmacological data available for a series of fentanyl analogs, in which the piperidine ring is conformationally restricted [30,31], seem to indicate that the piperidine ring is in the chair rather than the boat conformation in the active form of fentanyl.

These results clearly indicate the need of taking into account solvation effects in conformational studies, especially if the form in solution is charged (as in this case) through protonation.

Undoubtedly, a conformational study explicitly including the solvent molecules would be a more rigorous approach to the study of solvent effects on conformation. Such a study must include full geometry optimization of solvent and solute, which is very computer-intensive.

In this study, we found that one possible approach is to conduct an extensive conformational search of the molecule in its isolated state and then take into account the effect of the solvent environment on the lowest-energy conformers found in the search. The model chosen to simulate such effects, reoptimization with a different value of the dielectric constant, is quite crude but was sufficient to reverse the energy rank-ordering of the conformers. In agreement with the spectroscopic data, the CHARMm results with dielectric constants appropriate for chloroform and water indicate that the lowest-energy conformer in both solvents is a chair equatorial-equatorial (CEE).

The conformation of fentanyl recognized by the receptor, the so-called 'active' conformation, could be any of the five structures, CEE-α, CEE-V-β, CEA, BEA-H and CEE-I-α, found as low-energy forms, in water as well as in chloroform. In fact, they all lie within $\leqslant$4.5 kcal/mol from the minimum energy structure according to the CHARMm computations, and within $\leqslant$5.4 kcal/mol according to AM1. However, we can exclude the internally hydrogen-bonded boat as a candidate for the bioactive form on the following grounds: First of all, this structure is bound to be solvated in water and thus deprived of the stabilizing effect of the internal hydrogen bond. Moreover, we can assume that it reaches the receptor in its solvated form and then drops water of solvation to bind directly to the receptor. Thus, the results of these studies point to two basic possible structures of fentanyl as the bioactive form: a chair equatorial-equatorial (CEE) or a chair equatorial-axial (CEA).

The chair equatorial-axial (CEA) cannot be ruled out, at this point, at least not on energy grounds alone. Studies which are currently under way in our group on conformationally constrained fentanyl analogs will help assess the probability of this structure as a bioactive form.

One factor which has to be considered is the accessibility of this structure from the lowest-energy chair equatorial-equatorial. If the chair equatorial-equatorial really is the most stable conformer in solution, then the chair equatorial-axial can only be obtained from it through proton exchange with the solvent, in which the protonation occurs from the opposite side of the piperi-

dine ring. A temperature-dependent NMR study would help in determining the rate and the activation energy of the proton exchange of fentanyl with the solvent.

Both computational methods used favor, by a few kcal/mol, two different CEE structures rather than that obtained by optimizing the solid-state structure (Tables 7 and 8). These two chair equatorial-equatorial structures differ from the X-ray structure, either in the conformation of the phenethyl moiety (CEE-α) or in the conformation of the phenylpropanamide moiety (CEE-V-β).

One possible reason for the difference in stability between CEE-α and CEE-I-α could be attributed to the presence of stabilizing internal π–π interactions between the two phenyl rings in CEE-α. To a first approximation, we can assume that such an interaction occurs if the distance between the rings is smaller than or equal to the sum of the van der Waals radii of the carbon atoms on the rings (i.e., 3.6 Å). In the CHARMm-optimized CEE-α structure ($\varepsilon = 1$), the distance between the nearest carbon atoms on the two rings is 3.7 Å and the distance between the centers of the two benzene rings is 5.4 Å. Reoptimization with a different value of the dielectric constant further lengthens the latter distance to 6.3 Å ($\varepsilon = 78$) and 6.1 Å ($\varepsilon = 4.8$). Accordingly, we can rule out a π–π type of interaction as the stabilizing factor for the more favored CEE-α structure.

From the NMR and IR spectra [9], no clear-cut conclusion can be drawn about the conformation of the phenethyl side chain. The solid-state data indicate an extended conformation, corresponding to a value of $\tau_2 \approx 180°$. This conformation is also supported by structure–activity data of restricted naphthyl analogs of fentanyl [32]; in this case, though, the pharmacological data were obtained by in vivo experiments. As a consequence, it is difficult to separate the effects of a structural change from those due to differences in transport and metabolism.

In conclusion, the conformation CEE-α found by us as one of the two lowest-energy chairs equatorial-equatorial can very well coexist in solution with the conformation having the phenethyl side chain in extended arrangement.

For what concerns the plausibility of the conformer CEE-V-β as a bioactive form, we refer to pharmacological data on conformationally restricted spiro analogs of fentanyl [33]. These analogs, in which the anilido phenyl is forced to be in α- rather than in β-orientation, are highly potent, providing evidence that the same arrangement is probably favored in the active conformation of fentanyl. Also, the results of a 100-ps dynamics simulation run at 312 K ($\varepsilon = 78$), starting from the X-ray structure of fentanyl (data not published), show that the anilido phenyl oscillates in the α-arrangement and, for the whole length of the simulation, never assumes the β-arrangement. These results are a good indication that the energy barrier existing between α- and β-conformations cannot be overcome at physiological temperature.

On the basis of the pharmacological as well as the computational data, we thus feel we can rule out the chair equatorial-equatorial with β-arrangement of the anilido phenyl as active conformation.

It is interesting at this point to compare our results with those of two other conformational studies of fentanyl (Tollenaere et al. [16] and Froimowitz [19]). Tollenaere et al. considered only the chair conformation for the piperidine ring and the equatorial-equatorial arrangement of the substituents; thus we can only compare the CEE-α lowest-energy structure with their results. Moreover, they studied the conformational mobility of the phenylpropanamide and of the phenethyl moieties as separate fragments, so the comparison is necessarily done for the two separate sets of torsion angles φ_1, φ_2, φ_3 and τ_1, τ_2, τ_3, defining the conformational mobility of the phenylpropanamide and the phenethyl moieties, respectively.

For the phenylpropanamide substituent, the lowest-energy chair equatorial-equatorial found by us is very similar to one of the four isoenergetic minima found in the PCILO computations [16]. The only noticeable difference is in the value of the torsion angle φ_1 (our value: $-87.2°$; Tollenaere's value: $-130°$), our value being closer to the X-ray value ($\varphi_1 = -65.7°$). For the arylethyl moiety, our CEE structure also corresponds to one of the two calculated PCILO isoenergetic minima [16]. The torsion angle τ_1 which was kept fixed at 180° by Tollenaere et al. deviates as much as 25° from that value when left free to vary in our computations. It is interesting to notice that the PCILO computations predict a minimum for a value of τ_2 equal to $-50°$. This value is very close to the one found by us for the lowest-energy chair equatorial-equatorial ($\tau_2 = -39.9°$, CHARMm computations). Thus, the PCILO computations [16] also indicate the existence of a low-energy chair equatorial-equatorial conformation, in which the phenethyl moiety is not in the extended conformation.

The Froimowitz study [19] was conducted on the *N*-methyl analog of fentanyl, so no comparison is possible with our results for the phenethyl side chain. Concerning the phenyl propanamide moiety, Froimowitz pointed out that, on the basis of steric energy alone, this moiety can assume two energetically identical conformations, one the mirror image of the other, differing in the relative orientation of the phenyl ring and the carbonyl function with respect to the piperidine ring. In our computations, we also found two analogous conformations. However, due to the explicit consideration of the phenethyl substituent with high conformational flexibility, the energy of the two conformers was different (2–3 kcal/mol). The same low-temperature MD study mentioned above showed that, at physiological temperature, there is rapid interconversion between the two forms, so that they can be considered as indistinguishable for the purpose of defining the bioactive conformations.

CONCLUSIONS

Our conformational study of protonated fentanyl succeeded in locating 439 unique local minima. The global minimum found in the gas-phase approximation is an internally hydrogen-bonded boat, in disagreement with available experimental results from solution NMR and X-ray structures. However, simulation of solvent effects gave a chair equatorial-equatorial structure as the global minimum, consistent with the experimental data. This structure differs from the solid-state one in the orientation of the aromatic ring of the phenethyl substituent.

On energy grounds, either variation of the chair equatorial-equatorial conformers can represent the active conformation of fentanyl. A third candidate, within reachable energy range, is a chair with equatorial-axial 1,4 substituents. Further studies currently in progress with a set of fentanyl analogs are required to assess which of these are the most plausible bioactive forms.

The present study has shown that care must be taken when evaluating the results of gas-phase CHARMm computations of charged molecules, due to the probable overestimation of electrostatic interactions. One possible way of addressing this problem is simulation of the solvent effects by appropriate change of the dielectric constant in the CHARMm computations.

Calibration of the CHARMm results with those of higher-level quantum-mechanical computations such as AM1 can also help address this problem.

The conformational search strategy used, a combination of dihedral scans with MD simulations at two different temperatures, allowed the generation of many significantly different structures with very little overlap of similar conformers.

Analysis of the performance of the two techniques shows that the dihedral scan search procedure is sufficient for a complete analysis of the conformational space but only if all rotatable bonds are considered and sufficiently small increments of the angles are made. If these two criteria cannot be met in order to make the search amenable, MD simulations constitute an easy and fast way to explore the conformational space around a local minimum and/or to sample other conformational domains. However, on the basis of our results, we would not suggest the use of MD alone as a search technique for as complete an investigation as possible of the conformational space of small drug molecules.

ACKNOWLEDGEMENTS

Support for this work from NIDA Grant DA-02622 is gratefully acknowledged. We are thankful to one of the referees for drawing our attention to Dr. M. Froimowitz's publication and to Dr. M. Froimowitz himself for insightful discussion. One of us (C.C.-M.) would also like to thank Drs. J. Collins and H.O. Villar for many helpful discussions.

REFERENCES

1 Janssen, P.A., Br. J. Anaesth., 34 (1962) 260; U.S. Patent 3141823, Chem. Abstr., 62 (1964) 14634c.
2 James, I.F. and Goldstein, A., Mol. Pharm., 25 (1984) 337.
3 Yeadon, M. and Kitchen, I., In Progress in Opioid Research (NIDA Research Monograph 75), Rockville, MD, 1986.
4 Peeters, O.M., Blaton, N.M., De Ranter, C.J., Van Herk, A.M. and Goubitz, K., J. Cryst. Mol. Struct., 9 (1979) 153.
5 Peeters, O.M., Blaton, N.M. and De Ranter, C.J., Acta Crystallogr., B35 (1979) 999.
6 Koch, M.H.J., De Ranter, C.J., Rolies, M. and Dideberg, O., Acta Crystallogr., B32 (1976) 2529.
7 Michel, A., Lebrun, B., Evrard, G. and Durant, F., Acta Crystallogr., B38 (1982) 2961.
8 See references cited in Ref. 16.
9 Casy, A.F., Hassan, M.M.A., Simmonds, A.B. and Staniforth, D., J. Pharm. Pharmacol., 21 (1969) 434.
10 Brine, G.A., Boldt, K.G., Huang, P.-T., Sawyer, D.K. and Carroll, F.I., J. Heterocyclic Chem., 26 (1989) 677.
11 Cheney, B.V., Duchamp, D.J. and Christoffersen, R.E., In Barnett, G., Trsic, M. and Willette, R. (Eds.) QuaSAR Research Monograph 22, National Institute on Drug Abuse, Rockville, MD, 1978, p. 218.
12 Lobbezoo, M.W., Soudijn, W. and van Wijngaarden, I., Eur. J. Med. Chem.-Chim. Ther., 15 (1980) 357.
13 Feinberg, A.P., Creese, I. and Snyder, S.H., Proc. Natl. Acad. Sci. USA, 73 (1976) 4215.
14 Casy, A.F. and Parfitt, R.T., Opioid Analgesics, 1st edn., Plenum Press, New York, 1986, p. 487.
15 Lednicer, D. and Von Voigtlander, P.F., J. Med. Chem., 22 (1979) 1158.
16 Tollenaere, J.P., Moereels, H. and Van Loon, M., In Jucker, E. (Ed.) Progress in Drug Research, Vol. 30, Birkhäuser Verlag, Basel, 1986, p. 91.
17 Martin, J. and Andrews, P., J. Comput.-Aided Mol. Design, 1 (1987) 53.
18 Castiglione-Morelli, M.A., Lelj, F., Pastore, A., Salvadori, S., Tancredi, T., Tomatis, R., Trivellone, E. and Temussi, P.A., J. Med. Chem., 30 (1987) 2067.
19 Froimowitz, M., In Harris, L.S. (Ed.) Problems of Drug Dependence 1989 (NIDA Research Monograph 95), Rockville, MD, 1989, p. 302.
20 Brooks, B.R., Bruccoleri, R.E., Olafson, B.D., States, D.J., Swaminathan, S. and Karplus, M., J. Comp. Chem., 4 (1983) 187.
21 Polygen Corporation, 200 Fifth Ave., Waltham, MA 02254, U.S.A.
22 Dewar, M.J.S., Zoebisch, E.G., Healy, E.F. and Stewart, J.J.P., J. Am. Chem. Soc., 107 (1985) 3902.
23 MOPAC 5.0, QCPE Program 455, Bloomington, IN, U.S.A.
24 Shanno, D.F., J. Optimization Theory and Applications, 46 (1985) 87.
25 Fletcher, R. and Powell, M.D., Comput. J., 6 (1963) 163.
26 Karplus, M. and McCammon, J.A., Annu. Rev. Biochem., 52 (1983) 263.

27 McCammon, J.A. and Harvey, S.C., Dynamics of Proteins and Nucleic Acids, Cambridge University Press, Cambridge, 1987.
28 Merck Index, 11th edn., Merck and Co., Inc., Rakway, NJ, 1989.
29 Gasteiger, J. and Marsili, M., Tetrahedron, 36 (1980) 3219.
30 Riley, T.N. and Bagley, J.R., J. Med. Chem., 22 (1979) 1167.
31 Borne, R.F., Law, S.-J., Kapeghian, J.C. and Masten, L.W., J. Pharm. Sci., 69 (1980) 1104.
32 Fifer, E.K., Davis, W.M. and Borne, R.F., Eur. J. Med. Chem.-Chim. Ther., 19 (1984) 519.
33 Janssen, P.A., U.S. Patent 3155670, Chem. Abstr., 62P (1965) 7770f; Janssen, P.A., Fr. Patent M2986, Chem. Abstr., 63P (1965) 8372h.